Accommodation of vortices to columnar defects: Evidence for large entropic reduction of vortex localization

L. Krusin-Elbaum
IBM Research, Yorktown Heights, New York 10598-0218

L. Civale
Centro Atomico Bariloche—CNEA, 8400 Bariloche, Argentina

J. R. Thompson
Oak Ridge National Laboratory, Oak Ridge, Tennessee 37831
and Department of Physics, University of Tennessee, Knoxville, Tennessee 37996

C. Feild
IBM Research, Yorktown Heights, New York 10598-0218

(Received 26 September 1995; revised manuscript received 10 January 1996)

We map a pinning boundary in $YBa_2Cu_3O_{7-\delta}$ crystals with columnar defects via (i) a finite large drop of the persistent current $J(T)$, (ii) a maximum in the thermal relaxation rate $S(T)$, and (iii) the onset of $1/H$ field dependence of $J(H)$. This boundary is consistent with the ''accommodation'' field $B^{\star}(T)$ proposed by Nelson and Vinokur, separating the regime of vortices well localized on columnar pins from the interaction-dominated collective regime. The strong-pinning regime is limited by an unexpectedly low vortex depinning temperature $T_{dp}\sim 41$ K (below $0.5T_c$). [S0163-1829(96)01918-2]

I. INTRODUCTION AND BRIEF SUMMARY

It is now well accepted that columnar defects in a high-temperature superconductor pin magnetic vortices in the most efficient way.[1,2] The reason for the strong pinning is essentially topological—the vortex line can be confined over a considerable portion of its length L and thus can withstand a greater Lorentz force ($\propto L$). At low temperatures, the vortex matter in a material with columnar pins is expected to form a Bose-glass phase,[3] with vortices localized on these pins. For fields below the dose-equivalent matching field B_{Φ} (the field at which the densities of defects and vortices are equal), there are fewer vortices than pins and each vortex can find a columnar track by shifting over distances comparable to the mean separation between the defects. At low enough fields, vortex-vortex interactions are negligible and vortices will be pinned individually. In theory, this regime of strong single-vortex pinning (large critical current density J_c) is limited[3,4] in the $H-T$ plane by the ''accommodation field'' $B^{\star}(T)\leq B_{\Phi}$. Beyond this crossover boundary, collective effects become important and pinning is weaker.

Near zero temperature, $B^{\star}$ can be estimated by comparing the elastic energy loss due to the spatial adjustment with the gain in pinning energy.[3,4] As temperature increases *entropic* effects come into play and tend to oppose[3,4] the confinement of vortex cores inside a single track. This results in a decrease of the *effective* pinning energy by the entropic smearing factor $f(T/T_{dp})$, where $f(0)=1$ and $f(T)$ decreases with increasing temperature. The depinning temperature T_{dp}, a *single-track binding energy* beyond which the vortex line begins to wander away significantly from its columnar defect,[3] constrains the strong-pinning regime on the high-temperature side. Theoretical estimates[3,4] indicate that $T_{dp}\approx T_c(\nu/1+\nu)$, with $\nu=(r_0/4\xi_{ab}(0))(1/\sqrt{Gi})$. For the case of $YBa_2Cu_3O_{7-\delta}$ (YBCO), the Ginzburg number $Gi\sim 10^{-2}$, and the *ab*-plane coherence length $\xi_{ab}(0)\sim 12$ Å. Using the pin radius $r_0\sim 40$ Å (Ref. 5), we obtain $T_{dp}\sim 0.9T_c\sim 83$ K. This high depinning temperature suggests that $B^{\star}(T)$ should be relatively unaffected by entropic effects at low temperatures[3,4] (i.e., only weakly temperature dependent below $\sim 0.5T_c$).

In this paper we report an empirical pinning crossover in the $H-T$ diagram of columnar-defected YBCO crystals, which is consistent with the accommodation field $B^{\star}(T)$. This crossover is apparent from three distinctive features in the magnetic response, all of which were absent in the same crystals before irradiation. One feature is a large, almost steplike decrease in the persistent current density $J(T)$, which occurs below $0.5T_c$ and *only* for fields below B_{Φ}. Another characteristic is a *maximum* in the normalized creep rate $S(T)$, which coincides in the $H-T$ plane with the new feature in $J(T)$. Finally, we observe that on the high-field side of this crossover $J(H)$ is proportional to $1/H$, the field dependence expected in the collective-pinning regime of the Bose-glass phase.[3,4] The crossover field at $T=5$ K is nearly B_{Φ} and hence increases with irradiation dose, while the temperature scale does not depend on pin density. All these observations follow until the now untested theoretical expectations[3,4] for $B^{\star}$, except for the low value of the depinning temperature $T_{dp}\simeq 41$ K, which is well below expectations. A ''nonideal'' pinning efficiency of a real columnar defect allows easier wandering of vortices and thus a lower value of T_{dp}.

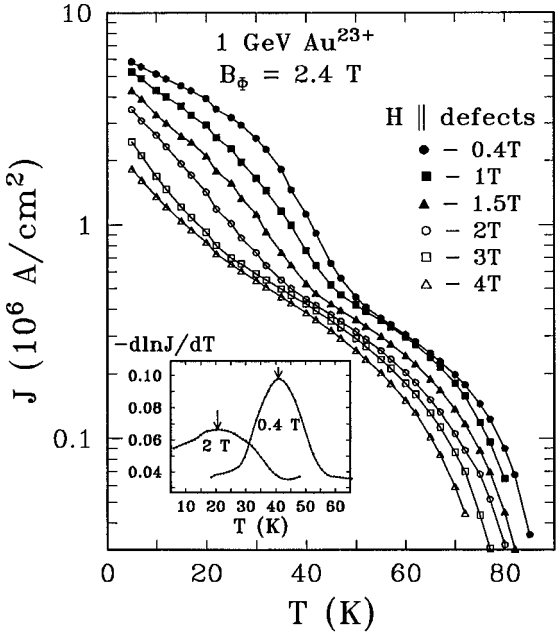

FIG. 1. Persistent current density $J(T)$ at several fields for a YBCO crystal irradiated with 1 GeV Au to a dose of 2.4 T. At low fields $J(T)$ shows a large reduction below $\sim 0.5T_c$. This is illustrated in the inset, where $-d\ln J/dT$ is shown to display a maximum which shifts to lower temperatures with increasing field and disappears at $\sim B_\Phi$.

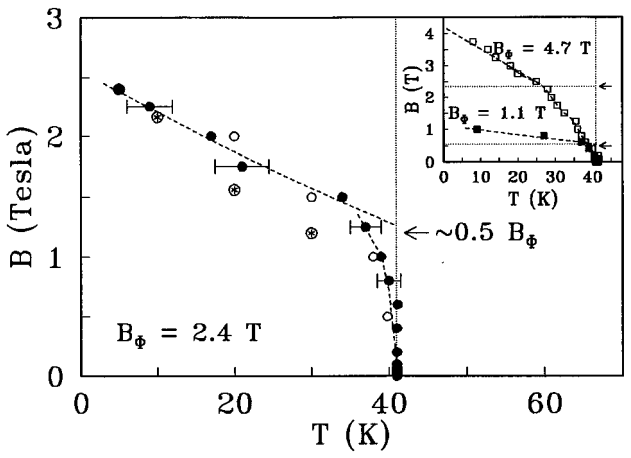

FIG. 2. $H-T$ phase diagram of YBCO crystals with parallel columnar defects. Accommodation field $B^\star(T)$ traced from the drop of the persistent current density $J(T)$ (maximum in $-d\ln J/dT$) for the crystal of Fig. 1 (solid dots). The maxima in the thermal relaxation rate $S(T)$ (displayed in Fig. 5) are plotted as open circles. $B^\star(T)$ decreases nearly linearly with T (extrapolating to zero at T_c) until it reaches $\sim 0.5B_\Phi$. At this field the there is also a crossover in the Bose-glass melting line (see Refs. 5 and 6). It drops abruptly at $T_{\rm dp} \simeq 41$ K. $T_{\rm dp}$ is dose independent, as shown in the upper inset for $B_\Phi = 1.1$ and 4.7 T. For large doses $B^\star(\sim 0\ \text{K}) < B_\Phi$ (see text). The values of $B^\star$ from scaling of *self-similar* $J(H/B^\star)$ are shown as encircled stars (see text and Fig. 4). The entropic smearing function is given by $f(T) = B^\star(T)/B^\star(0)$.

II. EMPIRICAL SIGNATURES OF THE "ACCOMMODATION" FIELD $B^\star(T)$

A. Experimental and measurement procedures

We studied several platelike YBCO crystals of ~ 1 mm size and ~ 20 μm thick along the c axis, irradiated with energetic (1.08 GeV) $^{197}Au^{23+}$ ions at the TASCC facility in Chalk River Laboratories, Canada. The ion beam was tilted off the c axis by 2° to avoid axial channeling and the dose rate was less than 8×10^8 ions/cm^2 sec to avoid heating.[5,6] To search for signatures of $B^\star(T)$ we examined the field, temperature and time dependence of the persistent current density $J(H,T,t)$ for several values of B_Φ. We obtained J from the irreversible magnetization $M(H,T,t)$ using the critical state model,[7] which relates J and M via a geometrical (shape) factor.[8] The magnetization was measured with a superconducting quantum interference device magnetometer in fields up to 5.5 T applied along the direction of the incident beam.

B. Large drop in persistent current density $J(T)$ at the "accommodation" field $B^\star(T)$

Figure 1 shows $J(T)$ for a YBCO crystal irradiated[5] to a dose of $B_\Phi = 2.4$ T for several values of field applied along the columnar tracks. The critical current density $J_c(H,T)$ is predicted to be high in the region of strongly localized, single-vortex pinning, and to decrease for fields above $B^\star$ due to vortex-vortex interactions.[3,4] We expect this decrease to be reflected in $J(T)$. The data of Fig. 1 clearly show that below B_Φ, the decrease in $J(T)$ with increasing temperature is initially *slow*, exhibits a *large drop at intermediate temperatures*, and slows down again at higher temperatures until the irreversibility line is approached.[9] The structure in $J(T)$ *is absent above* B_Φ and is unaffected by the crystal shape; i.e., two crystals with the same $B_\Phi = 2.4$ T but with a factor of 2 different aspect ratios, show an identical structure. We observe this effect in *all* irradiated crystals with pin densities from 0.6 to ~ 5 T. This behavior is distinctly different from the quasi-exponential temperature dependence universally seen at all fields in unirradiated crystals.[9] We choose to track the drop in $J(T)$ with the maximum slope in $\ln J$ vs T, i.e., with the maximum in $-d\ln J/dT$ vs T as illustrated in the inset of Fig. 1. The position of the maximum in $-d\ln J/dT$ for different values of magnetic field is plotted in Fig. 2. It traces a boundary in the field-temperature ($H-T$) plane which we denote $H_b(T)$.

At low temperatures $H_b \sim B_\Phi$, consistent with the theoretical expectation for $B^\star$. As T is increased, $H_b(T)$ decreases almost linearly and extrapolates to zero at $\sim T_c$. When $H_b(T)$ falls to $\sim 0.5B_\Phi$, it begins to decrease faster and becomes nearly *discontinuous* at $T \approx 41$ K. This limiting temperature is *independent of the irradiation dose* as demonstrated in the inset of Fig. 2, where equivalent data for two other crystals with $B_\Phi = 1.1$ and 4.7 T is shown. Our experimentally determined $H_b(T)$ follows a path in the $H-T$ plane consistent with $B^\star(T)$, and we interpret this *dose-independent* temperature as the *single-column* depinning temperature $T_{\rm dp}$. Strictly speaking, $B^\star(T)$ should be related to the position-dependent magnetic induction $B_b(T)$ and not to the external field $H_b(T)$. The difference, however, becomes appreciable only at fields below the self-field[10] induced by the persistent currents, $H_{\rm self}(T) \sim J(H_{\rm self},T)\,\delta/2$,

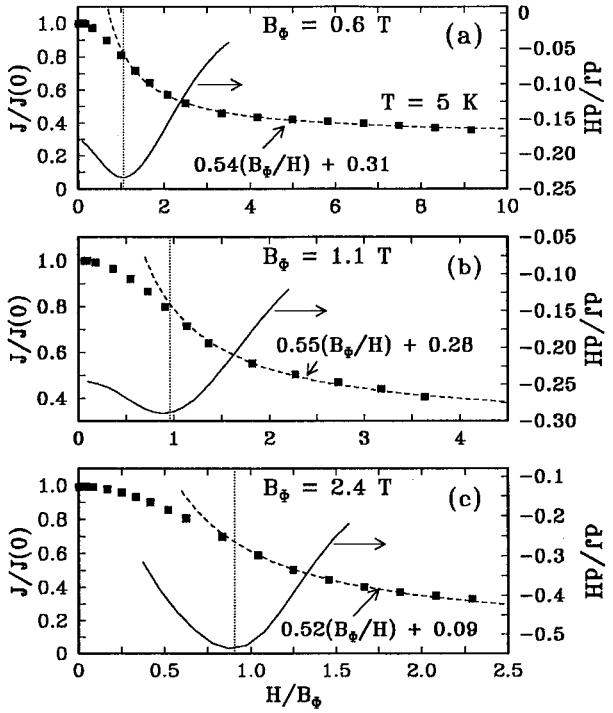

FIG. 3. $J(H)$ at 5 K [normalized to $J(0)$] vs H/B_Φ for YBCO crystals irradiated with 1 GeV Au with $B_\Phi=$ (a) 0.6 T, (b) 1.1 T, and (c) 2.4 T. We observe $1/H$ dependence indicative of collective pinning in all crystals above $B\simeq B_\Phi$, at which $|dJ/dH|$ (solid line) is largest.

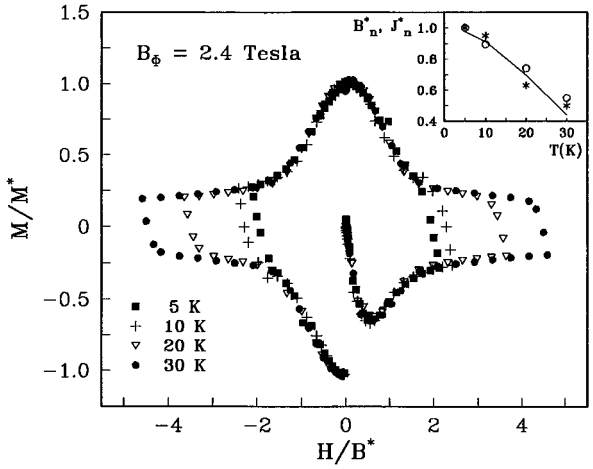

FIG. 4. Scaling of the magnetic hysteresis $M/M^\star=\mathrm{f}(H/B^\star)$ for the crystal of Fig. 1 at temperatures below $T_{\rm dp}$. We observe such self-similarity of $M(H)$ for all irradiation doses. The normalized values of scaling field $B_n^\star=B^\star(T)/B^\star$ (5 K) and current $J_n^\star=J^\star(T)/J^\star$ (5 K) are plotted in the inset as stars and open circles, respectively.

where δ is the crystal thickness. From the data in Fig. 2 we can estimate $H_{\rm self}(41\mathrm{K})\sim 1000$ Oe, well below the beginning of the abrupt decrease of $H_b(T)$, thus indicating that our determination of the depinning temperature $T_{\rm dp}$ is not affected by self-field effects. On the other hand, self-field effects preclude us from obtaining $B_b(T)$ below $H_{\rm self}(T)$, and consequently the predicted low-field tail in the accommodation field[3,4] above $T_{\rm dp}$ can be neither confirmed nor ruled out by the experiment. From now on we will focus on the regime $H>H_{\rm self}$ and thus we will disregard the differences between B and H.

The faster falloff of $B^\star(T)$ begins at nearly *half-filling* ($\sim 0.5B_\Phi$) for all doses. At higher doses the low-temperature value of $B^\star$ is reduced due to clustering of tracks in the ab plane as we discuss later.

C. Collective pinning above $B^\star(T)$: $1/H$ field dependence of $J(H)$

To verify our interpretation that $B^\star(T)=B_b(T)$, we need to establish the collective nature of pinning on the high-field side of B_b. *Above* $B^\star(T)$ the pinned objects are vortex bundles[3,4] and J_c is found by equating the Lorentz forces acting on *all* vortices and pinning forces acting only on *trapped* vortices[4]—we arrive at $J_c\propto 1/H$. Explicitly,

$$J_c(H,T)\simeq \alpha J_c(0,T)\frac{B^\star}{H}+J_c^{\rm pd},\quad B\geqslant B_\Phi, \tag{1}$$

where we have added $J_c^{\rm pd}$, the field-independent contribution from point defects, already present before irradiation.[1] Although we have no experimental access to J_c, at low temperatures, where the creep rates are small,[11] J is nearly J_c and thus the field dependence of $J(H,T)$ should approximately follow that of $J_c(H,T)$. So we first examine the 5 K data. The normalized $J(H)$ at this temperature for $B_\Phi=0.6$, 1.1, and 2.4 T is shown in Fig. 3. The fits to Eq. (1) are shown as dashed lines. The agreement is good for all doses, and the departure from the $1/H$ dependence at low fields occurs very near the field where $-dJ/dH$ is largest.[12] Thus, we identify the maximum slope change (solid line in Fig. 3) with $B^\star(T)$. This occurs almost exactly at B_Φ for $B_\Phi=0.6$ T. For larger doses, the inflection point shifts slightly downwards—it is at $H/B_\Phi\cong 0.92\pm 0.09$ for $B_\Phi=1.1$ T and $\cong 0.87\pm 0.1$ for a 2.4 T.

From the fits we obtain a prefactor $\alpha\simeq 1/2$, indicating that at $B^\star(T)$, about half of the vortices are pinned. This is an important piece of information that will be discussed in the context of pinning efficiency in Sec. III. The values of $J_c^{\rm pd}$ obtained from the fits are slightly larger than the values for the same crystals before irradiation. This can be easily understood by taking into account a small amount of random point defects generated as a ''side effect'' of the heavy-ion irradiation. We note that the predicted plastic pinning regime,[3] characterized by a $1/\sqrt{H}$ field dependence is not observed. This is consistent with the low $T_{\rm dp}$, which would preclude the appearance of the plastic regime, or at least shift it down to temperatures below those of our experiment.

From the onset of $1/H$ field dependence of $J(H)$ at 5 K, and following the same procedure at higher temperatures, we obtain an independent second estimate of $B^\star(T)$ also shown in Fig. 2. We know that this second estimate of $B^\star(T)$ will become progressively more unreliable as temperature increases due to the difference between J and J_c. Consistently, at 5 K we find an excellent agreement with B_b obtained earlier from $J(T)$, and less so at higher temperatures. We also find that $B^\star(T)$ can be used to scale the entire $J(H)$ at different temperatures, but *only below* $T_{\rm dp}$. Indeed, magnetic

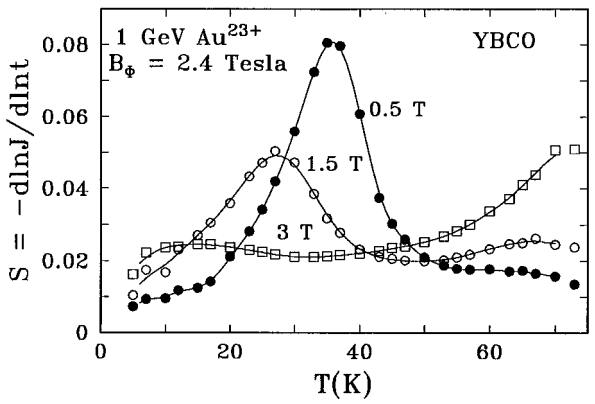

FIG. 5. Thermal relaxation rate $S(T)$ vs temperature for three values of applied field. $S(T)$ exhibits a peak for $H<B_\Phi$ which shifts towards lower temperatures as field is increased. It follows the boundary $B^\star(T)$ obtained from the peak in $d\ln J/dT$ (see Fig. 2 and the discussion in Sec. II D). The peak disappears in the collective-pinning regime above $B_\Phi=2.4$ T, as shown in the figure for $H=3$ T.

hysteresis loops are self-similar,[13] i.e., the shape of the hysteresis loops (or field dependence of the persistent current) is preserved under linear scaling transformation, as shown in Fig. 4. The scaling transformation can be written as $M/M^\star(T)=\mathrm{f}(H/B^\star(T))$ [or $J/J^\star=\mathrm{f}(H/B^\star)$]. The scaling field is $\sim B_\Phi$ at 5 K and it decreases by about 50% at 30 K as shown in the inset of Fig. 4 and in the $H-T$ diagram of Fig. 2. Above $T_{\rm dp}$, $J(H)$ is not monotonic, and the $M(H)$ loops are no longer self-similar.

D. Peak in the thermal relaxation rate

The maximum in $-d\ln J/dT$ suggests that a similar behavior may be found in the normalized thermal relaxation rate[4,9,14] $S=-d\ln J/d\ln t$. This is indeed observed, as shown in Fig. 5. We find a maximum in $S(T)$ which *occurs only for* $B<B_\Phi$, and closely follows the drop in J, i.e., the peaks in $d\ln J/dT$ and $S(T)$ occur essentially at the same temperature as marked by the open circles in Fig. 2. Our $S(T)$ data was obtained from the recorded time evolution ($60<t<7200$ sec) of $M(H,T,t)$ from the critical state.[9]

The basic reason for the similar behavior of $d\ln J/dT$ and S, is that in the collective pinning scenario,[4] time always appears in a combination $kT\ln(t/t_{\rm eff})$. This can be demonstrated more formally[15] as follows. We start with establishing the initial critical state at a temperature T. After a time t, the system has relaxed and adjusted so that the activation energy is $U=kT\ln(t/t_{\rm eff})$.[16] Since U is a function of the current density J which decreases with time, on very general grounds we can write[4] $U(T,J)=U_0(T)\mathbf{f}(J/J_c(T))$, where $U_0(T)$ is some characteristic energy scale and $\mathbf{f}$ is a decreasing function such that $\mathbf{f}(1)=0$. Hence, $J(T,t)=J_c(T)\mathbf{g}[y]$, where $\mathbf{g}$ is the inverse of $\mathbf{f}$ and $y=kT\ln(t/t_{\rm eff})/U_0(T)$. The relaxation rate $S(T)=-(d\mathbf{g}/dy)(dy/d\ln t)=-(d\mathbf{g}/dy)kT/U_0$. On the other hand, $d\ln J/dT=d\ln J_c/dT+(d\mathbf{g}/dy)(dy/dT)$ with $dy/dT=[kT\ln(t/t_{\rm eff})/U_0(T)][1/T-d\ln U_0/dT]$. By combining the above expressions we obtain

$$\frac{d\ln J}{dT}=\frac{d\ln J_c}{dT}-S(T)\ln(t/t_{\rm eff})\left[\frac{1}{T}-\frac{d\ln U_0}{dT}\right]. \qquad (2)$$

Equation 2 indicates that the features in $d\ln J/dT$ and $S(T)$ are strongly correlated. This is a natural consequence of the fact that both features have the same physical origin, namely a significant change in the J dependence of U upon crossing the accommodation field. Following the ideas of collective pinning,[4] in the regime of individual vortex pinning (below $B^\star$), the time relaxation of $J(H,T,t)$ will be fast and will slow down above $B^\star$ due to formation of vortex bundles.[4] Thus, by traversing the $H-T$ plane toward higher temperatures, we should find a decrease in the creep rate $S(T)$ when we cross $B^\star(T)$, as observed. A maximum is expected[4] from a prolific generation of double-kink excitations[11] near $T_{\rm dp}$. Above B_Φ, the creep rate is essentially flat in temperature and much lower (see Fig. 5), as expected in the regime of collective pinning.

III. LESS-THAN-IDEAL PINNING EFFICIENCY η OF COLUMNAR DEFECTS

A. Estimate of η at low temperatures

The pinning energy per unit length of a columnar track can be written as $U_p(T)\approx\eta f(T)\epsilon_0$, where $\epsilon_0=(\Phi_0/4\pi\lambda)^2$ is the line energy, λ is the magnetic penetration depth with currents in the ab plane,[3,4] and $f(T)$ is the entropic smearing factor of the pinning potential[3,4] discussed in Sec. I. The pinning efficiency $\eta\leqslant 1$ accounts for the ''nonideal'' nature of real defects; it absorbs all the numericals coming from the factor[3] $r_0/\xi_{ab}(0)$, the fractional suppression of the superconductivity in the defect,[1,5] and the *real* shape of the potential well. In the limit of noninteractive vortices (low fields), $J_c\sim cU_p(T)/\Phi_0\xi_{ab}\sim\eta f(T)J_0$, where J_0 is the depairing current density.[4] A rough estimate of η from the comparison of the optimal values of $J_c\cong 5\times10^7$ A/cm^2 in the irradiated YBCO crystals[1] and J_0 estimated at $\sim 3\times10^8$ A/cm^2 gives the single track pinning efficiency $\eta\sim 0.17$.

Let us now consider the low temperature limit [$f(T)\sim 1$] and analyze the dependence of $B^\star$ on η. In order to find a columnar pin (and gain energy U_p), a vortex will typically shift by $\sim d=\sqrt{\Phi_0/B_\Phi}$, at a cost of elastic energy per unit length $E_{\rm el}$. The simplest estimate gives $E_{\rm el}\sim C_{66}d^2$, where $C_{66}=\epsilon_0/4a_0^2$ is the local shear modulus of the vortex lattice[4] and $a_0=\sqrt{\Phi_0/B}$ is the vortex lattice spacing. At low fields $E_{\rm el}\ll U_p$ and pinning wins. Vortices will begin to wander when $E_{\rm el}\sim U_p$, leading to $B^\star(T\approx 0)\cong 4\eta B_\Phi$—clearly an unphysical result for $\eta>0.25$, since $B^\star$ cannot be larger than B_Φ. The origin of this is a non-negligible vortex *repulsion* near B_Φ, and thus the estimate of $E_{\rm el}$ must include a compression contribution[4] of the order $C_{11}d^2$. Since the above estimate is only correct for $B^\star<B_\Phi$, we infer that $B^\star(T)\sim 4\eta f(T)B_\Phi$ for $4\eta f(T)\ll 1$ and saturates at $\sim B_\Phi$ for larger values of η. From our data $B^\star(T\sim 0)\sim B_\Phi$ at low doses ($B_\Phi\leqslant 2.4$ T), implying $\eta\sim 0.25$, and smaller η values (consistent with our estimate obtained from J_c) for larger B_Φ.

The prefactor $\alpha\simeq 1/2$ in the field dependence of J [from the fits to Eq. (1) presented in Sec. II C] can now be understood with a straightforward statistical consideration. In the

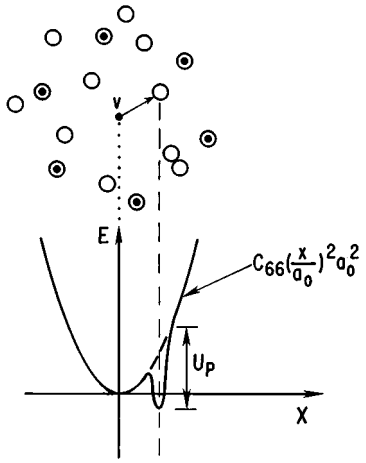

FIG. 6. Sketch of the competition between elastic and pinning energies of a vortex in a system of a random array of columnar pins. The vortex in the center (dot) will be pinned when it is within x_{cr} of the available defect (open circle).

absence of pinning vortices form a triangular lattice that can be divided in hexagonal unit cells of area $\sim a_0^2$ with a vortex at the center of each cell. Let us first consider the case of very strong pinning. In the regime $B<B_\Phi$, a vortex will be pinned provided that there is *at least one defect* within its hexagonal unit cell. In a sample of area A_s with only one columnar defect, the probability p of *not* having a defect in that cell is $p=(1-a_0^2/A_s)$. Here $A_s=a_0^2 N_\nu$, with N_ν being the total number of vortices; thus $p=(1-1/N_\nu)$. If the sample contains N_d defects, the probability P of *none* of them being in that area is a product of N_d independent probabilities: $P=(1-1/N_\nu)^{N_d}$. Using the relations $N_\nu\Phi_0=A_sB$ and $N_d\Phi_0=A_sB_\Phi$, we obtain $N_d=N_\nu(B_\Phi/B)$ and the probability of *pinning* the vortex becomes $P=1-P=1-[1-1/N_\nu]^{N_\nu(B_\Phi/B)}{}_{N_\nu\to\infty}\to 1-e^{-(B_\Phi/B)}$. Since J_c results from the balance between the Lorentz force acting on all the vortices and the pinning force acting only on pinned vortices, $J_c(B_\Phi)\cong J_c(0)\times P=0.63J_c(0)$, i.e., $\alpha\approx 0.63$.

For the case of nonideal defects, let us suppose that in order to find the nearest pin a vortex has to move by a distance x. This shift will result in a gain of pinning energy $U_p(T)\approx\eta f(T)\epsilon_0$ at a cost of elastic energy $C_{\rm el}x^2$. As we discussed earlier, the elastic constant $C_{\rm el}$ is some combination of the shear and bulk elastic moduli, C_{66} and C_{11}. The vortex will be pinned if there is a defect within the critical distance $x_{\rm cr}=\sqrt{U_p/C_{\rm el}}$ from its equilibrium position, as sketched in Fig. 6. The ''favorable'' area for pinning A_p, proportional to the pinning efficiency η, is now only a fraction of a_0^2. Since $B^\star/B_\Phi\propto\eta$, we can write $A_p\sim(B^\star/B_\Phi)a_0^2$, which gives the correct limit in the case of very strong pinning. If we now repeat the above derivation for this case, we find that the pinning probability becomes $P=1-e^{-(B^\star/B)}$; thus $J_c(B^\star)\cong 0.63J_c(0)$ and we recover $\alpha\approx 0.63$.

B. Entropic smearing function and low depinning temperature $T_{\rm dp}$

The experimentally determined entropic smearing is given by

$$f(T)=\frac{B^\star(T)}{B^\star(0)}. \tag{3}$$

We find that $f(T)$ clearly exhibits large reduction below $0.5T_c$ and a reduced value of $T_{\rm dp}$, as seen in Fig. 2. Both features are a natural consequence of the smaller pinning efficiency of the ''real'' columnar pins, not considered by the theory. Indeed, the experimental entropic factor cannot be directly compared with the existing models, since present theoretical estimates of entropic effects provide only limiting expressions:[3,4] i.e., $f(T)\propto 1-(T/T_{\rm dp})^2$ for $T\ll T_{\rm dp}$ and $f(T)\propto(T/T_{\rm dp})^2\exp[-(T/T_{\rm dp})^2]$ (short-range potential) or $f(T)\propto\exp[-(T/T_{\rm dp})]$ (long-range potential) for $T>T_{\rm dp}$, which depend sensitively on the range[4] and shape of the pinning well. No explicit prediction for $f(T)$ is available in the temperature region immediately below $T_{\rm dp}$. A particularly unexpected result is the abrupt character of the drop in $B^\star(T)$ [and thus in $f(T)$] immediately below $T_{\rm dp}$. Vortex dynamics in this region is complex[15] and it is not clear at this point if the sharp drop can be explained within the existing theoretical framework.

We can obtain a second independent estimate of $f(T)$ from the temperature dependence of J. In fact, at temperatures below $T_{\rm dp}$, J_c, and J should approximately obey the same scaling (see Sec. II C), since below $T_{\rm dp}$ and above $B^\star$ the creep rate is very weakly field dependent.[11] The scaling *current* is $J^\star(T)\propto J_c(0,T)\sim\eta f(T)J_0$ and thus should be $\propto B^\star(T)$, as we indeed observe (Fig. 4 inset).

IV. DECREASE OF PINNING EFFICIENCY AT HIGHER PIN DENSITIES DUE TO CLUSTERING OF TRACKS

Finally, we comment on the decrease of $B^\star$ at higher irradiation doses. This is essentially a problem of counting. Since the columnar tracks in the plane normal to the beam direction are randomly distributed, there will be tracks that overlap or nearly so. Here we present a very simple argument, which seems to reflect our experimental findings rather well. We start with N defects in an area A. Let us assume that within a cluster area $A_{\rm cl}=\pi r_{\rm cl}^2$ all tracks but one should be deleted from counting. The number of excluded defects $N'=\rho_\nu P$, where $\rho_\nu=B/\Phi_0$ is the vortex density, and probability of deletion $P=NA_{\rm cl}/2$. Thus the number of defects to be counted is $N_{\rm eff}=N-N'$ and the effective defect density $\rho_{\rm eff}=\rho_0(1-\rho_\nu A_{\rm cl}/2)$, where $\rho_0=B_\Phi/\Phi_0$. Obviously $\rho_{\rm eff}$ will be field dependent—the defect array will look more nonuniform with a few vortices than with lots of vortices. We take $B^\star(T\approx 0)$ to be a measure of $\rho_{\rm eff}$, i.e., $\rho_{\rm eff}=4\eta B_\Phi/\Phi_0$, and evaluate $\rho_{\rm eff}$ self-consistently at $\rho_\nu=\rho_{\rm eff}$. We immediately obtain $\rho_{\rm eff}/\rho_0=1/(1+\rho_0 A_{\rm cl}/2)$ or

$$4\eta=\frac{1}{1+\gamma B_\Phi}, \tag{4}$$

with $\gamma=A_{\rm cl}/2\Phi_0$. Figure 7 shows η [obtained from $B^\star(5{\rm K})\approx 4\eta B_\Phi$] vs B_Φ. From the fit to Eq. (4), we get the average cluster radius $r_{\rm cl}\sim 21$ nm, plausibly about five times the radius of the track.[5] The decrease of η at large B_Φ accounts for the optimum irradiation dose.[1]

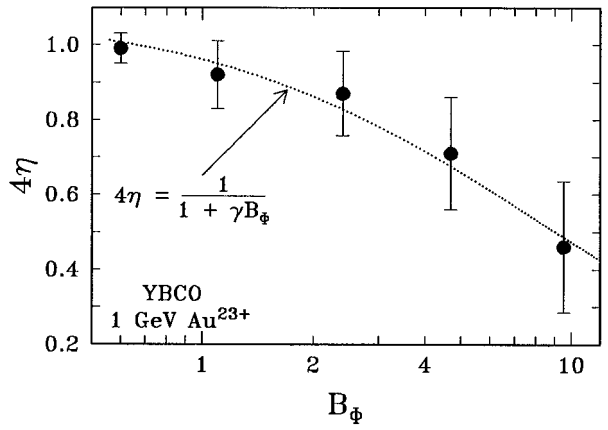

FIG. 7. Pinning efficiency η vs pin density B_Φ. The decrease of η at large values of B_Φ is due to clustering of pins randomly distributed in ab plane. The dotted line is the fit to Eq. (4), which recounts the effective pin density.

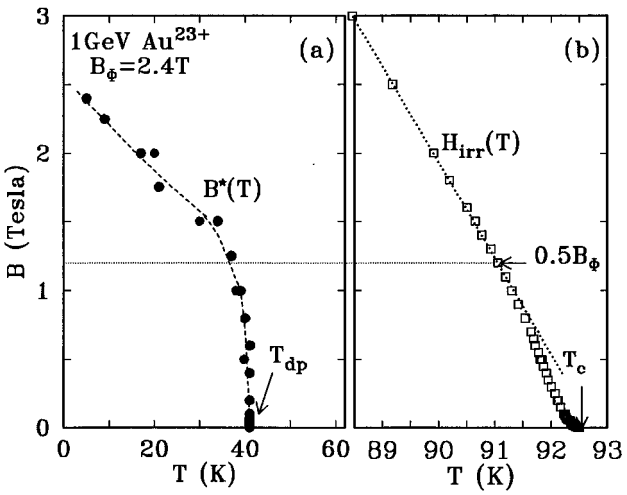

FIG. 8. $H-T$ phase diagram for vortices in YBCO with columnar defects ($B_\Phi = 2.4$ T). The Bose-glass melting line $B_{BG}(T)$ [approximated by $H_{irr}(T)$ at low fields] is from the ac susceptibility measurements (Ref. 5). Both the accommodation field $B^\star(T)$ (a) and $H_{irr}(T)$ (b) show a pronounced change in the behavior at about half the matching field ($\sim 0.5B_\Phi$).

V. CONCLUSION

In summary, we have drawn an experimental map of a new pinning boundary in the Bose-glass phase of a superconductor with columnar defects. We observe several independent features in pinning behavior, which converge to a single picture: a low-temperature regime with vortices strongly localized on columnar pins, followed by a crossover to a region of weak localization. This crossover from a single-vortex to collective-pinning regime is consistent with the ''accommodation'' field $B^\star(T)$, in accordance with the ideas of Nelson and Vinokur. We find the size of the strongly localized regime to be limited by a surprisingly low depinning temperature (less than half of T_c), indicating that there is a substantial entropic smearing of the pinning potential associated with columnar pins. The collective regime beyond T_{dp} is complex and low-field high-temperature vortex dynamics requires further exploration. The entire experimental $H-T$ diagram, including the Bose-glass melting line[5] is shown in Fig. 8. As we discussed in Sec. II B, $B^\star(T)$ begins to decrease very rapidly with increasing temperature at $\sim 0.5B_\Phi$. It is quite remarkable and probably not coincidental that the Bose-glass melting line $B_{BG}(T)$ also exhibits a crossover (kink) near half the matching field.[5,6] The entropic effects reduce the single-vortex regime for the real pins with less-than-ideal pinning efficiency more than is expected in the ideal case, a technologically important point since it is essential to understand the limits on strong pinning in high-T_c materials.

ACKNOWLEDGMENTS

We wish to acknowledge useful discussions with G. Blatter and V.M. Vinokur. We thank J. Hardy and J. Forster at TASCC (Chalk River, Canada) for their help and the provision of irradiation facilities. The operation of TASCC is supported by AECL Research. The research at ORNL was sponsored by the Division of Materials Sciences, USDOE under Contract No. DE-AC05-96OR22464 with Lockheed Martin Energy Research Corp.

[1] L. Civale, A.D. Marwick, T.K. Worthington, M.A. Kirk, J.R. Thompson, L. Krusin-Elbaum, Y. Sun, J.R. Clem, and F. Holtzberg, Phys. Rev. Lett. **67**, 648 (1991).

[2] M. Konczykowski, F. Rullier-Albenque, E.R. Jacoby, A. Shaulov, Y. Yeshurun, and P. Lejay, Phys. Rev. B **44**, 7167 (1991); R.C. Budhani, M. Suenaga, and S.H. Liou, Phys. Rev. Lett. **69**, 3816 (1992).

[3] D.R. Nelson and V.M. Vinokur, Phys. Rev. Lett. **68**, 2398 (1992); Phys. Rev. B **48**, 13 060 (1993).

[4] For a review, see, G. Blatter, M.V. Feigel'man, V.B. Geshkenbein, A.I. Larkin, and V.M. Vinokur, Rev. Mod. Phys. **66**, 1125 (1994).

[5] L. Krusin-Elbaum, L. Civale, G. Blatter, A.D. Marwick, F. Holtzberg, and C. Feild, Phys. Rev. Lett. **72**, 1914 (1994).

[6] L. Krusin-Elbaum, G. Blatter, and L. Civale, Phys. Rev. Lett. **75**, 187 (1995).

[7] A.M. Campbell and J.E. Evetts, Adv. Phys. **21**, 199 (1972).

[8] J.R. Clem and A. Sanchez, Phys. Rev. B **50**, 9355 (1994); in our case, for $J_c(5\text{ K}) \sim 7\times 10^6$ A/cm^2 and $t \sim 20$ μm, the characteristic field for a thin sample is $H_d = J_c t/2 \simeq 0.7$ T. Thus, with the maximum $H = 5.5$ T, the deviations from the conventional Bean model are insignificant.

[9] L. Civale, L. Krusin-Elbaum, J.R. Thompson, and F. Holtzberg, Phys. Rev. B **50**, 7188 (1994).

[10] M. Daeumling and D.C. Larbalestier, Phys. Rev. B **40**, 9350 (1989).

[11] L. Civale, L. Krusin-Elbaum, J.R. Thompson, R. Wheeler, A.D. Marwick, M.A. Kirk, Y. Sun, F. Holtzberg, and C. Feild, Phys.

Rev. B **50**, 4102 (1994); J.R. Thompson, L. Krusin-Elbaum, and L. Civale (unpublished).

[12] For fields $H \ll B^{\star}$, the vortex-vortex interaction is negligible and J_c is almost field independent, so that dJ_c/dH is almost zero. For $H \gg B^{\star}$, $J_c \propto B^{\star}/H$. The derivative with respect to H is $\propto 1/H^2$ and thus it decreases (in absolute value) with increasing H. It then follows that $|dJ/dH|$ *must* have a maximum with $B^{\star}/H$ being a natural field scale for this crossover.

[13] B.B. Mandelbrot, in *Fractal Geometry of Nature* (Freeman, New York, 1983).

[14] H.G. Schnack, R. Griessen, J.G. Lensink, and Wen Hai Hu, Phys. Rev. B **48**, 13 178 (1993).

[15] L. Civale, G. Pasquini, P. Levy, G. Nieva, D. Casa, and H. Lanza, Physica C (to be published).

[16] V.B. Geshkenbein and A. Larkin, Sov. Phys. JETP **68**, 639 (1989).